International Journal of General Medicine

Dovepress
Taylor & Francis Group

Open Access Full Text Article

ORIGINAL RESEARCH

MRI Parameters and Clinicopathologic Features in Predicting Hepatocellular Carcinomas With Aggressive-Related Marker Expression, Defined by Epithelial Cell Adhesion Molecule and Glypican-3 Status

YanZhuo Li[1,*], Lei Huo[2,*], LianLian Liu[1], NingYang Jia[2], Bin Song[1]

[1]Department of Radiology, Minhang Hospital, Fudan University, Shanghai City, 201100, People's Republic of China; [2]Department of Radiology, The Eastern Hepatobiliary Surgery Hospital, Naval Medical University, Shanghai City, 200438, People's Republic of China

*These authors contributed equally to this work

Correspondence: Bin Song, Department of Radiology, Minhang Hospital, Fudan University, No. 170, Xinsong Road, Shanghai City, 201100, People's Republic of China, Email songbin@fudan.edu.cn; NingYang Jia, Department of Radiology, The Eastern Hepatobiliary Surgery Hospital, Naval Medical University, No. 225, Changhai Road, Shanghai City, 200438, People's Republic of China, Email ningyangjia@163.com

Objective: Epithelial cell adhesion molecule (EpCAM) and glypican-3 (GPC3) are associated with a poor survival rate in hepatocellular carcinoma (HCC). Predicting aggressive HCC non-invasively should be investigated using preoperative gadoxetic acid-enhanced MRI and clinical characteristics.

Methods: This retrospective study examined 134 patients with confirmed cases of HCC who had undergone gadolinic acid-enhanced MRI before surgery. The data were collected between November 2017 and December 2021. Significant parameters were subjected to quantitative analysis and univariate testing. HCC characterized by poor differentiation and progenitor traits was identified by the positive expression of EpCAM and/or GPC3. Independent influencing variables for different subtypes of invasive HCC were identified by multivariate analysis. The diagnostic performance of variables was measured using ROC analysis.

Results: Cases with EpCAM and GPC3 expression were classified into four subtypes based on IHC staining. Among them, EpCAM +/GPC3+ HCC had the highest risk. Significant predictors of HCC expressing aggressive markers included tumor size ($p = 0.01$), AFP level ($p = 0.008$), MVI ($p = 0.003$), satellite nodule ($p = 0.002$), proliferative pattern ($p = 0.04$), and arterial peripheral enhancement ($p = 0.03$). By integrating all of these relevant variables, the resulting diagnostic accuracy was enhanced to 0.914 (95% CI 0.830–0.960) with a sensitivity of 0.964 (95% CI 0.922–1.000) and a specificity of 0.833 (95% CI 0.365–0.911).

Conclusion: The research demonstrated that combining biochemical and radiological data allows for accurate prognosis and patient management, along with non-invasive detection of aggressive HCC with high accuracy.

Keywords: glypican-3, epithelial cell adhesion molecule, hepatocellular carcinoma, magnetic resonance imaging

Introduction

Hepatocellular carcinoma (HCC) is associated with an increasing rate of cancer-related deaths.[1] Chronic hepatitis B virus (HBV) infection is the primary etiology for HCC in Asia and Africa.[2] Although detection and clinical treatment strategies have improved, and early intervention for liver cancer has been enhanced, the prognosis for HCC remains unfavorable due to frequent recurrence and metastasis.[1,2] HCC's prognosis is intimately associated with its biological features, with some less invasive cases possibly having a favorable outcome, while more invasive cases might have a dire prognosis.[1] Epithelial cell adhesion molecule (EpCAM), as one of the progenitor cell markers expressed in HCC, has been noted as a biomarker for cancer stem cells and is related to cancer proliferation, differentiation, migration, and invasion.[3,4]

Received: 22 October 2024
Accepted: 8 March 2025
Published: 26 March 2025

Furthermore, tumors expressing EpCAM positivity demonstrate aggressive biological characteristics and unfavorable outcomes, such as increased recurrence rates, resistance to radiation or chemotherapy, and a higher likelihood of metastasis.[3,4] Glypican-3 (GPC3) is involved in cellular growth, migration, differentiation, and invasion, as well as metastasis and recurrence in HCC.[1,5] Additionally, GPC3 is barely expressed in well-differentiated HCC and is never detected in cholangiocytes or cholangiocarcinomas.[6] GPC3 might be utilized as a diagnostic indicator for differentiation or as a tumor-specific marker in HCC,[6] and it is associated with poor prognosis.[7,8] Moreover, GPC3 can serve as an immunotherapeutic target in the treatment of HCC based on monoclonal antibodies.[7] These HCC show stemness or aggressiveness compared to conventional HCC with specific biomarkers (eg, increased frequency of MVI, decreased fibrous stroma and tumor pseudocapsule formation). These HCC are characterized by advanced stages, poor differentiation, and generally lower survival rates.[1]

Due to the varying etiological and genetic origins of HCC lesions, as well as the prolonged progression of the disease, there is considerable inter-and intra-tumor heterogeneity.[9] In HCC, therapeutic stratification is significantly complicated by tumor heterogeneity. However, given the intrinsic tumor heterogeneity, some analyses do not fully capture the exact state of the tumor. The diagnosis of HCC relies on tumor biopsy, yet the sensitivity is diminished by the size of the nodule and needle.[10] Therefore, more effective non-invasive strategies ought to be used to detect the early occurrence of HCC in high-risk groups,[11] including MRI and computed tomography, which may serve as surrogates for predicting specific molecular gene signatures.[12] Imaging can capture the entire tumor non-invasively, which is a significant advantage over genomics or histopathological analysis.[13] Analyzing tumor MRI features for heterogeneity can yield significant insights into the genetic, cellular, and molecular properties of tumors. This can lead to a deeper understanding of tumor features that play a crucial role in determining the most effective treatment options.[14] Despite histopathological and genetic heterogeneity in HCC tissues is well understood, imaging reports regarding the heterogeneity of HCC are extremely limited.[15] The imaging characteristics of HCC might differ depending on the presence or absence of precursor cell biomarkers, owing to their separate carcinogenic processes.[16] Because there is no certain clue what imaging features are present in EpCAM-positive HCC, imaging features of HCCs expressing EpCAM or GPC3 appear to overlap to some extent. According to the evidence at hand, only a few studies have concentrated on the MRI imaging features of HCC that test positive for EpCAM or GPC3. The research has mainly focused on the expression of either EpCAM or GPC3 alone, leading to inconsistent results.[17,18] Therefore, recent investigations have demonstrated that non-invasive MRI is valuable for assessing and estimating the invasiveness of HCC.

HCC with aggressive markers might have unique imaging traits compared to HCC without these markers. These differences could potentially indicate variations in tumor enhancement patterns, nodule form, and growth morphology. Additionally, the separate imaging information might further provide additional data on tumor properties, by combining imaging and histopathology data analysis, tumor characterization may be optimized, due to mutual information, which can facilitate predicting outcomes.[13] Effective treatment hinges on understanding this tumor form, with a primary focus on the role of radiological diagnosis. Identifying GPC3-positive and/or EpCAM-positive HCC early can offer significant clinical benefits for choosing treatments and evaluating the prognosis of HCC.

Despite advances in the diagnosis and treatment of HCC, there is still a significant clinical gap in predicting HCC with aggressive markers. In the clinical field, there is an absence of effective strategies to early and accurately identify HCC with abnormal and potentially aggressive EpCAM and GPC3. Therefore, the present study examined a variety of radiological and biological features and decided to explore the behavior of highly aggressive HCC. We aimed to investigate the relationship between EpCAM and GPC3 and the clinicopathologic features of HCC as well as MRI parameters, and to develop a comprehensive assessment system that can be used in the clinic, thus providing a basis for early clinical diagnosis, therapeutic decisions, and improved patient prognosis.

Materials and Methods

Patients and Tumors

A total of 263 patients who underwent preoperative gadolinium acetate-enhanced MRI and were pathologically diagnosed with HCC through resection between November 2017 and December 2021 in Minhang Hospital, Fudan

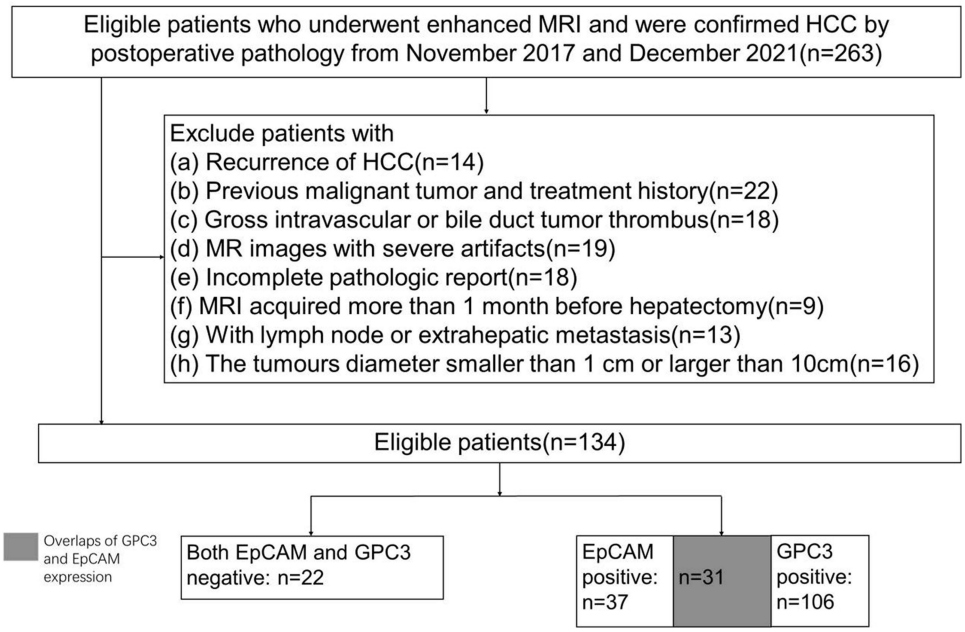

Figure 1 Flow diagram of the study population.

University were collected in this study. A retrospective examination identified 34 patients who were not included in the study because they did not undergo IHC staining for EpCAM and GPC3. The inclusion process of the study population is shown in Figure 1. Finally, a total of 134 patients with HCC were included in this study of which 112 were males and 22 were females. Participants had a mean age of 56.4 years, with ages ranging from 29 to 80. Inclusion criteria: (1) the whole tumor (satellites, and multicenter tumors; from the edge of the tumor margins ≥ 1 cm), had to be respectable; (2) patients met the Child-Pugh A liver function classification; and (3) preoperative imaging did not detect any indications of extrahepatic metastasis, large vessel invasion, gross bile duct tumor thrombosis, lymph node abnormalities, or extrahepatic metastasis; (4) Postoperative pathology reports were documented for all patients. Exclusion criteria: (a) MRI scan that dissatisfied the diagnostic criteria, (b) liver lesions with prior anticancer therapy before MRI examination, (c) MRI not obtained within 1 month before hepatectomy, (d) patients with other malignancies; (e) Incomplete histologic data, (f) Recurrence of HCC, and (g) Tumor diameter ≤ 1 cm or ≥ 10 cm. Baseline clinical information, including patient demographics and key laboratory test results, was collected from electronic medical records.

This trial was approved by the ethical committee of Minhang Hospital, Fudan University. This study's methodologies and procedures were all under ethical standards and local regulations.

Collection of Clinical Data

General data including age, gender, alpha-fetoprotein, protein induced by Vitamin K absence or antagonists-II (PIVKA-II) and HBsAg levels before hepatectomy were collected from all patients.

Liver MRI Protocol and Assessment

All MRI scans were conducted via the GE Signa Infinity Twinspeed 1.5 T with an 8-channel abdominal coil. Before the scan, all participants fasted for 4 hours and received breathing instructions. Routine liver MRI was performed within 1–2 weeks before surgical resection: breath-hold, axial T1-weighted dual-echo gradient-recalled echo (GRE) (repetition time [TR]/echo time [TE] =185.9/4.3 ms, 256×170 matrix, 7-mm slice thickness); a turbo spin-echo sequence with fat suppression T2-weighted (TR/TE = 7059/105.6 ms, 320×224 matrix, 7-mm slice thickness). In the median cubital veins of the patients, a high-pressure syringe was used to administer gadoxetic acid-enhanced imaging (Primovist; Bayer Berlin Germany) at a dose of 0.1 mmoL/kg. A 20 mL saline flush was then administered after the injection. To obtain an axial T1-weighted three-dimensional (3D) GRE, fat suppression (Liver Acquisition with Volume Acceleration, LAVA) was

used in combination with dynamic contrast-enhanced imaging to acquire images of the arterial phase (AP), portal venous phases (PVP), delayed phases (DP), and hepatobiliary phase (HBP) at 22 to 25s, 50 to 60s, 90 to 120s, and 20 min, respectively.

The MR images were reviewed and extracted from the PACS by two abdominal radiologists (H.L. and Y.L., with 10 to 15 years of experience in liver imaging). The reviewers also independently evaluated tumor hallmarks as follows: (1) tumor margin (clear or vague margin in HBP images); (2) tumor shape (characteristics oval or irregular in HBP images); (3) tumor size; (4) radiologic capsule; (5) arterial rim enhancement; (6) arterial peritumoral enhancement on AP; (7) peritumoral hypointensity on HBP; (8) dynamic enhancement pattern (which include arterial enhancement with wash-out, arterial and continuous enhancement, gradually increase, and no or minimum enhancement); (9) T1-weighted and HBP imaging (hypo-, iso-, and hyperintensity). Both radiologists independently documented the presence or absence of these results in each distinct set of images. After the first independent image analyses, the two readers maintained more than 2 weeks in image assessment to reduce recall bias. In discordant cases, a consensus was adjusted by asking a senior radiologist for consultation and finally coming to a consistent conclusion.

Pathology and Immunohistochemistry Features

The largest target lesion was selected among multiple lesions, like satellite lesions. All cases were examined by a senior pathologist (Sw P). Along with a junior pathologist (Lian L). Histopathological factors were assessed, including tumor size and number, growth type, histological grade, proliferation pattern, capsule formation status, presence of satellite nodules, MVI, hemorrhage or necrosis, and the variety of cirrhosis. The larger diameter of the tumor specimen was used to quantify its size. Growth patterns were identified as simple nodular, infiltrative, multifocal nodular confluent, massive and simple nodular with extranodular.

Immunoreactivity expression of GPC3 and EpCAM was reviewed by experienced pathologists. The positive percentage (%) for each marker was used to quantify immunoreactivity. The presence of GPC3 and EpCAM immunoreactivities were categorized as either negative ($\leq$ 5% of tumor cells) or positive ($\geq$ 5% of tumor cells). The above-mentioned macroscopic and microscopic histopathological variables, along with imaging features, especially the positivity or negativity of these markers, were evaluated based on the immunoreactivity outcome for GPC3 or EpCAM. According to the IHC staining results, the patients were categorized into four different subgroups: EpCAM+/GPC3+ (Group A), EpCAM−/GPC3+ (Group B), EpCAM+/GPC3− (Group C), and EpCAM−/GPC3− (Group D).

Classifications of Histopathological Factors

The histological grade was categorized as I, II, III, or IV as per the Edmondson–Steiner nuclear grading scheme. Tumor grades were determined by identifying the predominant grade present within the tumor when multiple grades coexisted. The proliferation pattern was defined as macrotrabecular, microtrabecular, clear cell, pseudoglandular, compact, or scirrhous. Capsule formation status was classified as relatively intact, partially penetrated, or completely absent. Further satellite nodules were observed within a 2 cm proximity to the primary HCC lesion. Microvascular invasion refers to the occurrence of tumor thrombi within small peritumoral vessels, such as the portal vein, hepatic vein, hepatic artery, or other microvessels. A variety of cirrhosis was categorized as normal hepatic parenchyma, micronodular, mixed-nodular, and macronodular cirrhosis.

Statistical Analysis

Continuous parameters were presented as means ± SD and medians (range), and categorical values were expressed as counts (%), as appropriate. Clinical and imaging features were compared according to the final immunoreactivity diagnoses of the 134 patients' pathological review by using ANOVA or Kruskal Wallis tests for continuous variables and Fisher's exact test or Chi-Square test for categorical variables, followed by pairwise categories according to immunoreactivity findings ("HCC with GPC3 (+)" vs "HCC with GPC3 (−)", "HCC with EpCAM (+)" vs "HCC with EpCAM (−)") for each marker. P values for trend were employed for overall comparisons because alterations in clinical and imaging features due to immunoreactivity expression were of clinical importance. Then, pairwise comparisons between the adjacent histologic categories were only performed when P values for trend were $\geq$ 0.05. All groups (Groups

A, B, C, and D) were compared based on the results of the combined immunoreactivity of EpCAM and GPC3 to determine the overall difference between HCC with and without invasive marker expression. Because four possible pairs of adjacent categories were compared, P values ≤ 0.05/4 (0.013) were regarded as statistically significant when the Bonferroni correction was applied. Univariable and multivariable logistic regression analyses with significant variables ($p \leq 0.05$) were used to identify the predictors of GPC3 or EpCAM expressing HCC. ROC analyses were performed to evaluate the utility of quantitative parameters to discriminate immunoreactivity markers. The threshold for statistical significance was a two-sided *p*-value of ≤ 0.05. Areas under the receiver operating characteristic curve were obtained for each factor in the presence of immunopositive findings, and sensitivity, specificity, positive predictive value, negative predictive value, and accuracy with corresponding 95% CI were determined. The statistical analyses were conducted with the software of IBM SPSS Statistics 23.0.

Results

Demographic and Pathologic Characteristics of HCC for EpCAM and GPC3 Expression

There were 134 patients with a male-to-female ratio of 112 to 22, with an age (mean ± SD) of 56.44 ± 10.06 years. The mean diameter of the lesions was 4.09 ± 1.98 cm. About 118 patients had only one lesion and the remaining 16 patients had two or more lesions. Chronic hepatitis was the most predominant cause of the underlying liver disease (85.8% of patients), including 112 patients with B viral infection and 3 patients with C viral infection. By using immunohistochemistry, we examined the expression of EpCAM and GPC3 in all 134 primary HCC. Table 1 summarizes the details of the immune responses of the study participants. Positive EpCAM expression was detected in 37 out of 134 HCC cases (27.6%). Of the 134 HCC cases, 106 were positive for GPC3 (79.1%). The patients were grouped according to EpCAM and GPC3 expression in the two HCC groups, and the clinical and histopathologic analyses of the patients were compared, as shown in Table 2. Overall, patients with GPC3 and EpCAM-positive HCC cases had higher serum AFP levels ($p = 0.000$, $p = 0.02$, respectively). And GPC3-positive HCC cases showed more frequent aggressiveness in proliferation patterns ($p = 0.05$). In other pathologic analyses, EpCAM-positive HCC cases had a higher frequency of MVI ($p \leq 0.01$) than EpCAM-negative HCC cases. No significant differences were noted between the EpCAM or GPC3 expression groups in any other clinicopathological features.

Based on the expression of EpCAM and GPC3, all 134 HCC cases were classified into four immuno-subtypes: (1) EpCAM+/GPC3+ (Group A), 31 cases (23.1%); EpCAM−/GPC3+ (Group B), 75 cases (56.0%); EpCAM+/GPC3− (Group C), 6 cases (4.5%); EpCAM−/GPC3− (Group D), 22 cases (16.4%), respectively (Table 3). All subtypes were predominantly seen in men, but no statistically significant difference in the distribution of gender was detected between any two subtypes of HCC. The average incidence age of EpCAM−/GPC3− HCC was older, and the AFP and PIVKA-II levels were lower than those of the other subtypes, but, there were no substantial variations observed between any two subtypes of HCC ($p \geq 0.05$). As for serum AFP level, three grades were conducted as ≤ 20 ng/mL, 20 to 400 ng/mL, and ≥ 400 ng/ mL. EpCAM−/GPC3− HCC showed the least cases with AFP levels above 400 ng/ mL. Whereas, EpCAM +/GPC3+ and EpCAM−/GPC3+ HCC cases were clinically characterized by higher serum AFP levels (p =0.01), which could further suggest the aggressiveness of HCC (Table 3).

Table 1 Immunoreactivities for GPC3 and EpCAM

	EpCAM (+)	EpCAM (−)	Total
Immunoreactivity findings			
GPC3 (+)	31	75	106 (79.1%)
GPC3 (−)	6	22	28 (20.9%)
Total	37 (27.6%)	97 (72.4%)	134

Note: Data represent the number of patients.
Abbreviations: EpCAM, epithelial cell adhesion molecule; GPC3, Glypican-3.

https://doi.org/10.2147/IJGM.S502309

Table 2 Clinical and Imaging Features of EpCAM and GPC3 Diagnoses

Characteristic	EpCAM			GPC3		
	Positive (n = 37)	**Negative (n = 97)**	**P value**	**Positive (n = 106)**	**Negative (n = 28)**	**P value**
Demographic and Serum Characteristics						
Gender			0.19			0.566
Male	28(75.7%)	84(86.6%)		87(82.1%)	25(89.3%)	
Female	9 (24.3%)	13(13.4%)		19(17.9%)	3 (10.7%)	
Age (a, years)	56.76 ± 7.37	56.32 ± 10.94	0.823	55.66 ± 10.47	59.39 ± 7.78	0.081
PIVKA-II (b, mAU/mL).	129(15–17,589)	137(10–20,961)	0.811	139(14–19,183)	113(10–20,961)	0.822
AFPL (3%, a)	22.95 ± 18.89	16.86 ± 14.02	0.161	18.81 ± 15.91	19.25 ± 17.20	0.949
Hepatitis			0.676			1
Present	31(83.8%)	84(86.6%)		91(85.8%)	24(85.7%)	
Absent	6(16.2%)	13(13.4%)		15(14.2%)	4(14.3%)	
AFP (ng/mL, a)	361.86 ± 76.83	178.68 ± 35.80	**0.016**	261.55 ± 39.62	107.01 ± 59.73	0.65
AFP (ng/mL)			0.67			**0.000**
< 20	12(32.4%)	49(50.5%)		39(36.8%)	22(78.6%)	
20–400	15(40.5%)	36(40.5%)		47(44.3%)	4(14.3%)	
> 400	10(27.0%)	12(12.5%)		20(18.9%)	2(7.1%)	
Histopathological Characteristics						
Diameter of main nodule (cm)			0.153			0.114
≤ 2	4(10.8%)	16(16.5%)		18(17.0%)	2(7.1%)	
2–3	12(32.4%)	17(17.5%)		26(24.5%)	3(10.7%)	
3–5	9(24.3%)	38(39.2%)		36(34.0%)	11(39.3%)	
5–10	12(32.4%)	26(26.8%)		26(24.5%)	12(42.9%)	
Diameter of main nodule (cm, a)	3.82 ± 1.69	4.20 ± 2.08	0.308	3.95 ± 2.08	4.64 ± 1.49	0.101
Nodule number			0.377			1
1	31(83.8%)	87(89.7%)		13(12.3%)	3(10.7%)	
1 < n	6(16.2%)	10(10.3%)		93(87.7%)	25(89.3%)	
Microvascular invasion			**0.01**			0.585
Present	22(59.5%)	27(27.8%)		40(37.7%)	9(32.1%)	
Absent	15(40.5%)	70(72.2%)		66(62.3%)	19(67.9%)	
Satellite nodule			0.19			0.557
Present	17(45.9%)	66(68.0%)		67(63.2%)	16(57.1%)	
Absent	20(54.1%)	31(32.0%)		39(36.8%)	12(42.9%)	
Cirrhosis Type			0.960			0.865
Normal liver	23(62.2%)	61(62.9%)		67(63.2%)	17(60.7%)	
Micronodular	7(18.9%)	19(19.6%)		21(19.8%)	5(17.9%)	
Mixednodular	7(18.9%)	15(15.5%)		16(15.1%)	6(21.4%)	
Macronodular	0(0.0%)	2(2.1%)		2(1.9%)	0(0.0%)	
Edmondson-Steiner grade			1			0.188
I	0(0.0%)	1(1.0%)		0(0.0%)	1(3.6%)	
II	3(8.1%)	10(10.3%)		9(8.5%)	4(14.3%)	
III	33(89.2%)	83(85.6%)		93(87.7%)	23(82.1%)	
IV	1(2.7%)	3(3.1%)		4(3.8%)	0(0.0%)	
Hemorrhage or necrosis			0.213			0.362
Present	34(91.9%)	81(83.5%)		89(84.0%)	26(92.9%)	
Absent	3(8.1%)	16(16.5%)		17(16.0%)	2(7.1%)	
Pericancerous capsule			0.82			0.553
Absent	11(29.7%)	14(14.4%)		19(17.9%)	6(21.4%)	
Partially penetration	25(67.6%)	81(83.5%)		85(80.2%)	21(75.0%)	
Relatively intact	1(2.7%)	2(2.1%)		2(1.9%)	1(3.6%)	

(*Continued*)

Table 2 (Continued).

Characteristic	EpCAM			GPC3		
	Positive (n = 37)	**Negative (n = 97)**	**P value**	**Positive (n = 106)**	**Negative (n = 28)**	**P value**
Proliferation pattern			0.17			**0.05**
Microtrabecular	1(2.7%)	6(6.2%)		4(3.8%)	3(10.7%)	
Macrotrabecular	25(67.6%)	83(85.6%)		90(84.9%)	18(64.3%)	
Clear Cell	4(10.8%)	1(1.0%)		2(1.9%)	3(10.7%)	
Scirrhous	3(8.1%)	2(2.1%)		3(2.8%)	2(7.1%)	
Compact	3(8.1%)	3(3.1%)		5(4.7%)	1(3.6%)	
Pseudoglandular	1(2.7%)	2(2.1%)		2(1.9%)	1(3.6%)	
Growth type			0.143			0.089
Simple nodular	12(32.4%)	28(28.9%)		35(33.0%)	5(17.9%)	
Simple nodular with extranodular growth	7(18.9%)	9(9.3%)		14(13.2%)	2(7.1%)	
Multifocal nodular confluent	7(18.9%)	24(24.7%)		26(24.5%)	5(17.9%)	
Massive	8(21.6%)	34(35.1%)		27(25.5%)	15(53.6%)	
Infiltrative	3(8.1%)	2(2.1%)		4(3.8%)	1(3.6%)	
Morphologic MRI Characteristics						
Tumor shape			0.295			0.211
Oval	17(45.9%)	35(36.1%)		62(58.5%)	20(71.4%)	
Irregular	20(54.1%)	62(63.9%)		44(41.5%)	8(28.6%)	
Tumor margin			0.08			0.242
Clear	20(54.1%)	68(70.1%)		67(63.2%)	21(75.0%)	
Vague	17(45.9%)	29(29.9%)		39(36.8%)	7(25.0%)	
T1-weighted imaging			0.465			0.390
Hypointensity	85(87.6%)	33(89.2%)		95(89.6%)	23(82.1%)	
Isointensity	7(7.2%)	4(10.8%)		8(7.5%)	3(10.7%)	
Hyperintensity	5(5.2%)	0(0.0%)		3(2.8%)	2(7.1%)	
Arterial rim enhanced			**0.03**			0.567
Present	11(29.7%)	9(9.3%)		15(14.2%)	5(17.9%)	
Absent	26(70.3%)	88(90.7%)		91(85.8%)	23(82.1%)	
Peritumoral-enhanced on AP			0.997			0.288
Present	8(21.6%)	21(21.6%)		25(23.6%)	4(14.3%)	
Absent	29(78.4%)	76(78.4%)		81(76.4%)	24(85.7%)	
Enhancement pattern			**0.027**			0.110
Arterial enhancement with wash-out	25(67.6%)	83(85.6%)		88(83.0%)	20(71.4%)	
Arterial and continuous enhancement	2(5.4%)	6(6.2%)		4(3.8%)	4(14.3%)	
Gradually increase	3(8.1%)	1(1.0%)		4(3.8%)	0(0.0%)	
No or minimum enhancement	7(18.9%)	7(7.2%)		10(9.4%)	4(14.3%)	
Enhancing capsule			0.474			0.355
Present	11(29.7%)	23(23.7%)		25(23.6%)	9(32.1%)	
Absent	26(70.3%)	74(76.3%)		81(76.4%)	19(67.9%)	
HPB intensity			0.129			0.583
Hypointensity	34(91.9%)	95(97.9%)		101(95.3%)	28(100%)	
Hyperintensity	3(8.1%)	2(2.1%)		5(4.7%)	0(0.0%)	
Peritumoral hypointensity on HBP			**0.021**			0.368
Present	19(51.4%)	29(29.9%)		40(37.7%)	8(28.6%)	
Absent	18(48.6%)	68(70.1%)		66(62.3%)	20(71.4%)	

Notes: unless indicated otherwise, data are number of patients, and data in parentheses are percentages. P value of ≤ 0.05 and values labeled in bold format indicates a statistically significant difference. a data are mean values ± standard deviation; b data are median values and data in parentheses are ranges.

Abbreviations: AFP, alpha-Fetoprotein; PIVKA-II, Protein induced by Vitamin K absence or antagonists-II; MRI, Magnetic resonance imaging; HBP, Hepatobiliary phase.

Table 3 Clinicopathologic and Imaging Characteristics Regarding Different HCC Subtypes Defined by EpCAM and GPC3 Expression

Characteristic	No.	Immuno-subtype				P value for trend*
		Group A (n = 31)	Group B (n = 75)	Group C (n = 6)	Group D (n = 22)	
Demographic and Serum Characteristics						
Gender						0.389
Male	112	23(20.5%)	64(57.1%)	5(4.5%)	20(17.9%)	
Female	22	8(36.4%)	11(50.0%)	1(4.5%)	2(9.1%)	
Age (years, a)	134	56.68 ± 7.13	55.24 ± 11.59	57.17 ± 9.24	60.00 ± 7.46	0.278
PIVKA-II (mAU/mL, b)	134	99(15–17,589)	145(10–20,961)	149.5(40–768)	54(14–19,183)	0.876
AFPL (3%, a)	134	21.94 ± 19.11	17.41 ± 14.32	28.70 ± 20.30	9.80 ± 7.72	0.387
Hepatitis						0.506
Present	115	27 (23.5%)	64(55.7%)	4(3.5%)	20(17.4%)	
Absent	19	4(21.1%)	11(57.9%)	2(10.5%)	2(10.5%)	
AFP (ng/mL, a)	134	381.61 ± 84.57	211.93 ± 42.84	259.8 ± 194.64	65.34 ± 54.70	**0.033**
AFP (ng/mL)						**0.01**
< 20	61	9(14.8%)	30(49.2%)	3(4.9%)	19(31.1%)	
20–400	51	13(25.5%)	34(66.7%)	2(3.9%)	2(3.9%)	
> 400	22	9(40.9%)	11(50.0%)	1(4.5%)	1(4.5%)	
Histopathological Characteristics						
Diameter of main nodule (cm)						0.234
≤ 2	20	4(20.0%)	14(70.0%)	0(0.0%)	2(10.0%)	
2–3	29	11(37.9%)	15(51.7%)	1(3.4%)	2(6.9%)	
3–5	47	7(14.9%)	29(61.7%)	2(4.3%)	9(19.1%)	
5–10	38	9(23.7%)	17(44.7%)	3(7.9%)	9(23.7%)	
Diameter of main nodule (cm,a)	134	3.66 ± 1.73	4.07 ± 2.21	4.62 ± 1.35	4.65 ± 1.56	0.060
Nodule number						0.395
1	118	25(21.2%)	68(57.6%)	6(5.1%)	19(16.1%)	
1 < n	16	6(37.5%)	7(43.8%)	0(0.0%)	3(18.8%)	
Microvascular invasion						**0.008**
Present	49	19(38.8%)	21(42.9%)	3(6.1%)	6(12.2%)	
Absent	85	12(14.1%)	54(63.5%)	3(3.5%)	16(18.8%)	
Satellite nodule						0.087
Present	83	14(16.9%)	53(63.9%)	3(3.6%)	13(15.7%)	
Absent	51	17(33.3%)	22(43.1%)	3(5.9%)	9(17.6%)	
Cirrhosis Type						0.970
Normal liver	84	19(22.6%)	48(57.1%)	4(4.8%)	13(15.5%)	
Micronodular	26	6(23.1%)	15(57.7%)	1(3.8%)	4(15.4%)	
Mixednodular	22	6(27.3%)	10(45.5%)	1(4.5%)	5(22.7%)	
Macronodular	2	0(0.0%)	2(100.0%)	0(0.0%)	0(0.0%)	
Edmondson-Steiner grade						0.605
I	1	0(0.0%)	0(0.0%)	0(0.0%)	1(100.0%)	
II	13	2(15.4%)	7(53.8%)	1(7.7%)	3(23.1%)	
III	116	28(24.1%)	65(64.9%)	5(4.3%)	18(15.5%)	
IV	4	1(25.0%)	3(75.0%)	0(0.0%)	0(0.0%)	
Hemorrhage or necrosis						0.359
Present	115	28(24.3%)	61(53.0%)	6(5.2%)	20(17.4%)	
Absent	19	3(15.8%)	14(73.7%)	0(0.0%)	2(10.5%)	
Pericancerous capsule						0.306
Absent	25	8(32.0%)	11(44.0%)	3(12.0%)	3(12.0%)	
Partially penetration	106	22(20.8%)	63(59.4%)	3(2.8%)	18(17.0%)	
Relatively intact	3	1(33.3%)	1(33.3%)	0(0.0%)	1(33.3%)	

(*Continued*)

Table 3 (Continued).

Characteristic	No.	Immuno-subtype				P value for trend*
		Group A (n = 31)	Group B (n = 75)	Group C (n = 6)	Group D (n = 22)	
Proliferation pattern						**0.003**
Microtrabecular	7	1(14.3%)	3(42.9%)	0(0.0%)	3(42.9%)	
Macrotrabecular	108	23(21.3%)	67(62.0%)	2(1.9%)	16(14.8%)	
Clear Cell	5	2(40.0%)	0(0.0%)	2(40.0%)	1(20.0%)	
Scirrhous	5	2(40.0%)	1(20.0%)	1(20.0%)	1(20.0%)	
Compact	6	2(33.3%)	3(50.0%)	1(16.7%)	0(0.0%)	
Pseudoglandular	3	1(33.3%)	1(33.3%)	0(0.0%)	1(33.3%)	
Growth type						0.344
Simple nodular	65	13(20.0%)	39(60.0%)	2(3.1%)	11(16.9%)	
Simple nodular with extranodular growth	16	6(37.5%)	8(50.0%)	1(6.3%)	1(6.3%)	
Multifocal nodular confluent	31	6(19.4%)	20(54.5%)	1(3.2%)	4(12.9%)	
Massive	17	3(17.6%)	7(41.2%)	2(11.8%)	5(29.4%)	
Infiltrative	5	3(60.0%)	1(20.0%)	0(0.0%)	1(20.0%)	
Morphologic MRI Characteristics						
Tumor shape						0.474
Oval	82	16(19.5%)	46(56.1%)	4(4.9%)	16(19.5%)	
Irregular	52	15(28.8%)	29(55.8%)	2(3.8%)	6(11.5%)	
Tumor margin						0.239
Clear	88	16(18.2%)	51(58.0%)	4(4.5%)	17(19.3%)	
Vague	46	15(32.6%)	24(52.2%)	2(4.3%)	5(10.9%)	
T1-weighted imaging						0.666
Hypointensity	118	28(23.7%)	67(56.8%)	5(4.2%)	18(15.3%)	
Isointensity	11	3(27.3%)	5(45.5%)	1(9.1%)	2(18.2%)	
Hyperintensity	5	0(0.0%)	3(60.0%)	0(0.0%)	2(40.0%)	
Arterial rim enhanced						**0.011**
Present	20	8(40.0%)	7(35.0%)	3(15.0%)	2(10.0%)	
Absent	114	23(20.2%)	68(59.6%)	3(2.6%)	20(17.5%)	
Peritumoral-enhanced on AP						0.785
Present	29	7(24.1%)	18(62.1%)	1(3.4%)	3(10.3%)	
Absent	105	24(22.9%)	57(54.3%)	5(4.8%)	19(18.1%)	
Enhancement pattern						**0.049**
Arterial enhancement with wash-out	108	22(20.4%)	66(61.1%)	3(2.8%)	17(15.7%)	
Arterial with continuous enhancement	8	1(12.5%)	3(37.5%)	1(12.5%)	3(37.5%)	
Gradually increase	4	3(75.0%)	1(25.0%)	0(0.0%)	0(0.0%)	
No or minimum enhancement	14	5(35.7%)	5(35.7%)	2(14.3%)	2(14.3%)	
Enhancing capsule						0.313
Present	34	10(29.4%)	15(44.1%)	1(2.9%)	8(23.5%)	
Absent	100	21(21.0%)	60(60.0%)	5(5.0%)	14(14.0%)	
HPB intensity						0.224
Hypointensity	129	28(21.7%)	73(56.6%)	6(4.7%)	22(17.1%)	
Hyperintensity	5	3(60.0%)	2(40.0%)	0(0.0%)	0(0.0%)	
Peritumoral hypointensity on HBP						0.091
Present	48	17(35.4%)	23(47.9%)	2(4.2%)	6(12.5%)	
Absent	86	14(16.3%)	52(60.5%)	4(4.7%)	16(18.6%)	

Notes: EpCAM+/GPC3+ (Group A); EpCAM−/GPC3+ (Group B); EpCAM+/GPC3− (Group C); EpCAM−/GPC3− (Group D). Unless indicated otherwise, data are number of patients, and data in parentheses are percentages. a data are mean values ± standard deviation; b data are median values and data in parentheses are ranges; AFP alpha-Fetoprotein; PIVKA-II Protein induced by Vitamin K absence or antagonists-II; MRI Magnetic resonance imaging; HBP Hepatobiliary phase. * P values for trend were calculated by using ANOVA analysis of variance for continuous variables and the χ^2 test for categorical variables. P values less than 0.05 and values labeled in bold format indicate statistical significance.

Among the four subtypes, EpCAM+/GPC3+ HCC demonstrated the highest frequency of MVI (19/31, 61.2%), and EpCAM+/GPC3− subtype had a frequency of 50% (3/6), which was significantly higher than EpCAM−/GPC3+ (21/75, 28.0%) and EpCAM−/GPC3− (6/22, 27.3%) groups. Tumors with macrotrabecular pattern accounted for 80.60% (108/134) of all subtypes of HCC, which demonstrated a higher proportion than that of other histological variants in all groups ($p \leq 0.01$). Macrotrabecular variants that indicate aggressive features accounted for 74.19% (23/31) and 89.33% (67/75) of EpCAM+/GPC3+ and EpCAM−/GPC3+ cases, respectively. EpCAM−/GPC3+ HCC cases were more likely to have a macrotrabecular pattern than the other 5 variants ($p \leq 0.05$). And EpCAM−/GPC3− HCC cases were more likely to present in the microtrabecular pattern, which mimicked the normal hepatic plates without statistical significance. A strong correlation was observed between the immunosubtype and morphological classification of HCC, as shown in Table 3. Lesion aggressiveness was inversely proportional to the diameter of the lesion (p =0.06). Nevertheless, a high proportion of EpCAM−/GPC3+ HCCs (64.9%) was at stage III, showing higher positive rates for fibrous capsule penetration and lower incidence of hemorrhage or necrosis, which depict a higher ratio than other subtypes, although the differences did not reach statistical significance (p = 0.605, 0.306, and 0.359, respectively) (Table 2). For the growth type of the tumor, the multifocal nodular confluent type was more commonly seen (72.2%) in EpCAM−/GPC3+ HCC, while EpCAM−/GPC3− HCC was associated with low invasiveness simple nodular type; however, no significant difference existed according to any of the five growth types ($p \geq 0.05$).

Qualitative Image Analysis

Qualitative analyses were demonstrated in Table 2. Combining MRI and growth morphology parameters in a 50-year-old male patient with confirmed EpCAM-positive HCC (Figure 2F), EpCAM-positive HCC lesions show mildly heterogeneous hypodense lesions with fibrosis (Figure 2A), exhibiting a trend toward enhancement of the arterial margins (P = 0.03) (Figure 2B-D). Regarding enhancement pattern, typical arterial enhancement with a wash-out pattern was more common in EpCAM-negative HCC, while EpCAM-positive HCC showed atypical enhancement patterns more frequently (p = 0.027). As for peritumoral hypointensity on HBP, it was significantly more common in HCC with EpCAM-positive

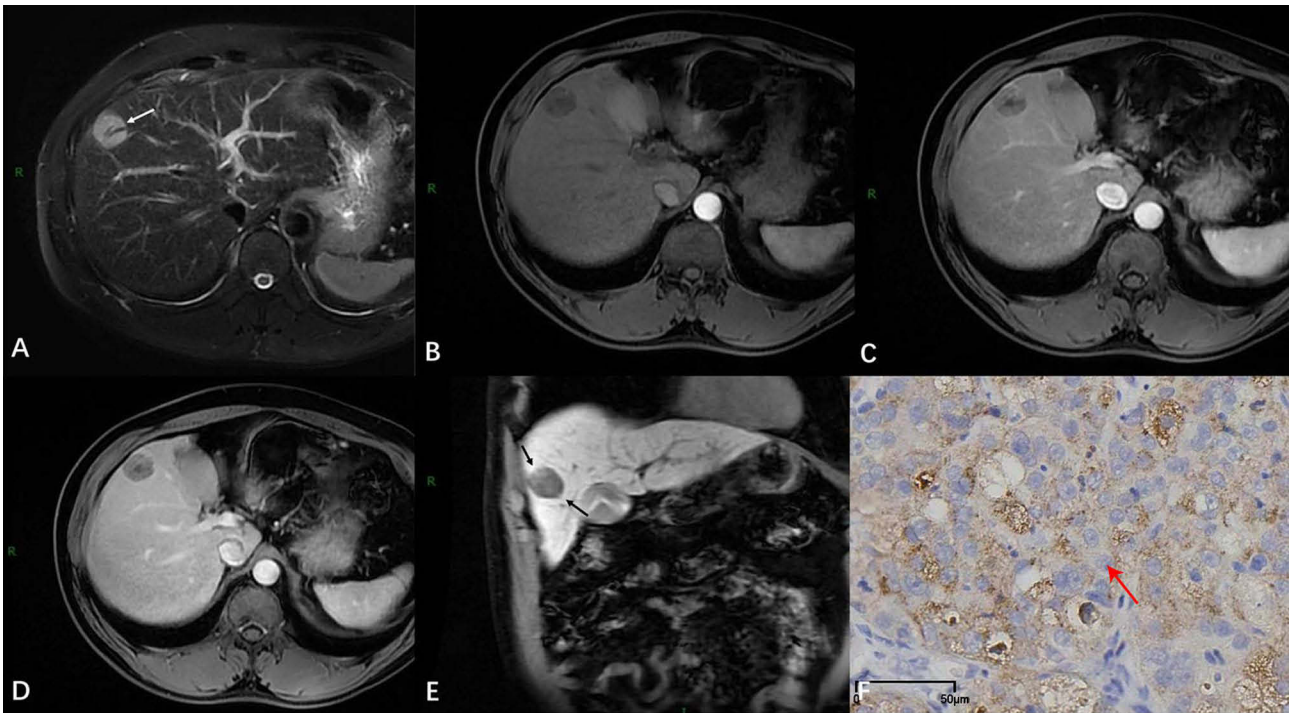

Figure 2 HCC presenting with EpCAM positive expression in a 50-year-old man. (**A**) T2WI showed a slightly heterogeneous hypointense lesion with fibrotic intensity (white arrow). (**B-D**) The lesion showed no enhancement on AP, slight rim enhancement on PVP (black arrow), and unclear margin and unevenly hypointense on DP. (**E**) On the HBP image, the lesion is hypointense with partially vague margin and shows a peripheral budding (black arrow). (**F**) Immunoreactivity was positive for EpCAM.

expression (p = 0.021) (Figure 2E). Other morphological features were equally observed in HCC with and without EpCAM and GPC3 expression (Table 2). We further assessed the image characteristics of the 4 subtypes of HCC. Statistical difference was also observed in rim enhancement between these four subtype groups (p =0.011), while hardly being seen in other MRI features. In terms of dynamic enhancement pattern, arterial enhancement with wash-out was more common in EpCAM+/GPC3+ and EpCAM−/GPC3+ HCC (p = 0.049) than in GPC3-negative HCC. The prevalence of peritumoral hypointensity on HBP in HCC showed no significance between groups (p = 0.091). As an example, on MRI of a 32-year-old male patient with HCC diagnosed as GPC3-positive (Figure 3F), the lesion was moderately dense and accompanied by a slight blurring of the demarcation in the liver parenchyma (Figure 3A), demonstrating fuzzy margins and heterogeneous enhancement of the periampullary envelope (Figure 3B-D), and peritumoral hypodensities were demonstrated on HBP (Figure 3E).

In the pairwise comparisons, according to Table 4, EpCAM+/GPC3+ HCC differed from EpCAM−/GPC3+ in MVI, satellite nodule, arterial rim enhancement, arterial enhancement with wash-out, and peritumoral hypointensity on HBP ($p \leq 0.05$). The differences in macrotrabecular and cell pattern, arterial rim enhancement, and arterial enhancement with wash-out between EpCAM+/GPC3− and EpCAM−/GPC3+ groups were statistically significant. In addition, the difference in serum AFP level between EpCAM+/GPC3+ and EpCAM−/GPC3− groups was also significant. Other pairwise comparisons, including those between EpCAM+/GPC3− and EpCAM−/GPC3−, did not reveal differences in any of the analyses ($p \geq 0.05$, Table 4).

The Linear-by-Linear Association test revealed that the rates of serum AFP level, MVI, satellite nodule involvement, macrotrabecular and cell pattern, typical enhancement, and arterial rim enhancement grew considerably together with the transformation of phenotype from EpCAM−/GPC3− to EpCAM−/GPC3+, then EpCAM+/GPC3+ (for all p-trend ≤ 0.01). These findings demonstrated a strong correlation between the immunosubtype and the malignancy of HCC. The most aggressive subtype of HCC was EpCAM+/GPC3+, which was followed by EpCAM−/GPC3+. The least aggressive subtype of HCC was EpCAM−/GPC3−.

Table 5 summarizes the results of the univariable and multivariable logistic regression analysis to select features for differentiating EpCAM−/GPC3−, EpCAM−/GPC3+, and EpCAM+/GPC3+ HCC. Multivariable analysis revealed that

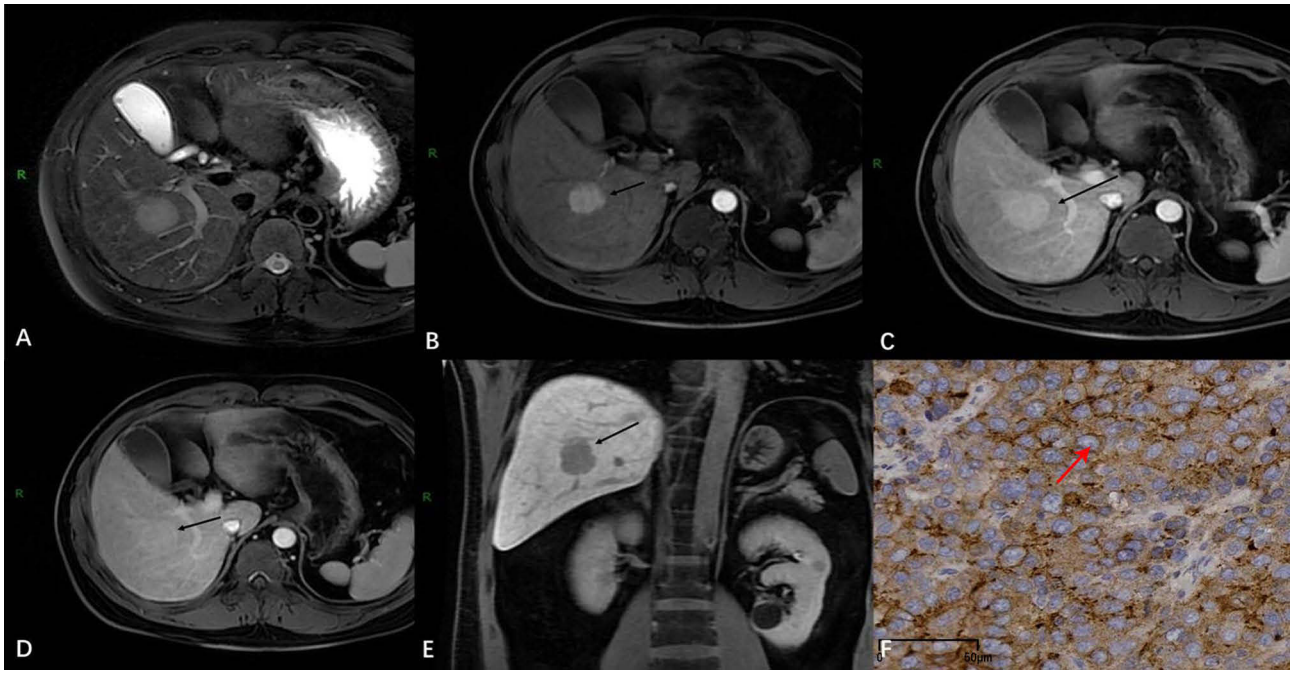

Figure 3 HCC presenting with GPC3 positive expression and an atypical enhancement pattern in a 32-year-old man. (**A**) The lesion is moderately hyperintense on T2WI and slightly vague-delineated in the liver parenchyma; (**B-D**) It shows clear gross enhancement on AP, vague margin on PVP and DP, and unevenly enhancing capsule. (**E**) On the HBP image, the lesion is hypointense with irregular shape. (**F**) Immunoreactivity was positive for GPC3.

https://doi.org/10.2147/IJGM.S502309

Table 4 The Correlation Clinical and Imaging Features Between Any Two Immuno subtype of HCC

Parameter	Post Hoc Analysis (P value)			
	A versus B	**B versus C**	**C versus D**	**A versus D**
Tumor diameter (cm)	F = 1.457 P > 0.05	F = 0.023 P > 0.05	F = 0.087 P > 0.05	F = 4.357 P = 0.042
AFP (ng/mL)	F = 3.901 P > 0.05	F = 0.089 P > 0.05	F = 1.840 P > 0.05	**F = 8.171 P = 0.006**
AFP (ng/mL)				
< 20	χ^2 = 1.135 P > 0.05	χ^2 = 0.230 P > 0.05	χ^2 = 3.702 P > 0.05	**χ^2 = 16.973 P < 0.000**
20–400	χ^2 = 3.025 P > 0.05	χ^2 = 0.331 P > 0.05	χ^2 = 3.702 P > 0.05	**χ^2 = 16.909 P < 0.000**
> 400	χ^2 = 2.957 P > 0.05	χ^2 = 0.018 P > 0.05	χ^2 = 1.044 P > 0.05	χ^2 = 4.564 P = 0.037
Microvascular invasion	**χ^2 = 10.346 P = 0.001**	χ^2 = 1.290 P > 0.05	χ^2 = 1.116 P > 0.05	χ^2 = 5.975 P = 0.025
Satellite nodule	**χ^2 = 6.136 P = 0.013**	χ^2 = 1.112 P > 0.05	χ^2 = 0.159 P > 0.05	χ^2 = 0.999 P > 0.05
Proliferation pattern				
Microtrabecular	χ^2 = 0.036 P > 0.05	χ^2 = 0.249 P > 0.05	χ^2 = 0.916 P > 0.05	χ^2 = 1.999 P > 0.05
Macrotrabecular	χ^2 = 3.923 P > 0.05	**χ^2 = 13.805 P = 0.004**	χ^2 = 3.187 P > 0.05	χ^2 = 0.014 P = 0.041
Clear Cell	χ^2 = 4.932 P > 0.05	**χ^2 = 25.633 P = 0.005**	χ^2 = 4.084 P > 0.05	χ^2 = 0.088 P > 0.05
Scirrhous	χ^2 = 2.089 P > 0.05	χ^2 = 1.899 P > 0.05	χ^2 = 1.044 P > 0.05	χ^2 = 0.088 P > 0.05
Compact	χ^2 = 1.324 P > 0.05	χ^2 = 0.081 P > 0.05	χ^2 = 3.802 P > 0.05	χ^2 = 2.257 P > 0.05
Pseudoglandular	χ^2 = 0.424 P > 0.05	χ^2 = 12.656 P = 0.014	χ^2 = 0.283 P > 0.05	χ^2 = 0.062 P > 0.05
Arterial rim enhanced	χ^2 = 4.899 P = 0.027	**χ^2 = 8.490 P = 0.004**	χ^2 = 5.379 P = 0.05	χ^2 = 2.349 P > 0.05
Enhancement pattern				
Arterial enhancement with wash-out	χ^2 = 4.514 P = 0.047	**χ^2 = 6.357 P = 0.012**	χ^2 = 1.718 P > 0.05	χ^2 = 0.263 P > 0.05
Arterial and continuous enhancement	χ^2 = 0.036 P > 0.05	χ^2 = 1.899 P > 0.05	χ^2 = 0.035 P > 0.05	χ^2 = 1.999 P > 0.05
Gradually increase	χ^2 = 4.206 P > 0.05	χ^2 = 0.081 P > 0.05	NA	χ^2 = 2.257 P > 0.05
No or minimum enhancement	χ^2 = 2.299 P > 0.05	χ^2 = 5.004 P > 0.05	χ^2 = 2.263 P > 0.05	χ^2 = 0.556 P > 0.05
Peritumoral hypointensity on HBP	χ^2 = 6.454 P = 0.019	χ^2 = 0.019 P > 0.05	χ^2 = 0.085 P > 0.05	χ^2 = 3.981 P > 0.05

Notes: EpCAM+/GPC3+ (Group A); EpCAM−/GPC3+ (Group B); EpCAM+/GPC3− (Group C); EpCAM−/GPC3− (Group D). P values are for pairwise comparisons between the adjacent two categories when P values for trend in overall comparisons were significant. P values less than 0.013 and values labeled in bold format were regarded as indicating statistical significance. Adjusted using Bonferroni correction.

higher AFP level, MVI, and smaller tumor size were associated with EpCAM+/GPC3+ (odds ratios, 15.82[95% CI: 1.26, 199.44], 0.01 [95% CI: 0.00, 0.31], 18.41 [95% CI: 1.93, 175.20], respectively; P values of 0.008, 0.007, and 0.01, respectively; Table 5), compared with EpCAM−/GPC3− HCC. EpCAM+/GPC3+ HCC showed more frequency with

Table 5 Univariate and Multivariate Logistic Regression Analyses of Variables in Predicting Between Any Two Immuno subtype of HCC

Characteristic	Univariate Analysis		Multivariate Analysis	
	OR (95.0% CI)	**P value**	**OR (95.0% CI)**	**P value**
A versus B				
Tumor diameter (cm)	1.03(0.99–1.06)	0.08		
AFP (ng/mL)	1.0 (0.99–1.0)	0.08		
MVI	0.78(0.01–0.42)	**0.003**	0.10(0.02–0.46)	**0.003**
Satellite Nodule	10.09(1.92–52.98)	**0.006**	8.88(2.19–36.11)	**0.002**
Proliferation pattern	11.75(0.45–307.37)	0.78		
Arterial rim enhancement	4.02(0.10–161.49)	0.46		
Enhancement pattern	0.71(0.01–70.86)	0.25		
Peritumoral hypointensity on HBP	0.53(0.15–1.92)	0.34		
B versus C				
Tumor diameter (cm)	1.02(0.97–1.08)	0.41		
AFP (ng/mL)	1.0 (0.99–1.0)	0.66		
MVI	22.89(0.59–885.59)	0.09		

(*Continued*)

Table 5 (Continued).

Characteristic	Univariate Analysis		Multivariate Analysis	
	OR (95.0% CI)	P value	OR (95.0% CI)	P value
Satellite Nodule	10.09(1.92–52.98)	0.18		
Proliferation pattern	3.11(1.06–9.14)	**0.04**	0.07(0.01–0.91)	**0.04**
Arterial rim enhancement	113.66(1.0–12,930.42)	**0.05**	15.82(1.26–199.44)	**0.03**
Enhancement pattern	0.56(0.10–3.04)	0.50		
Peritumoral hypointensity on HBP	0.91(0.06–13.58)	0.95		
A versus D				
Tumor diameter (cm)	17.87(1.84–169.96)	**0.01**	18.41(1.93–175.20)	**0.01**
AFP (ng/mL)	0.06 (0.01–0.38)	**0.002**	15.82(1.26–199.44)	**0.008**
MVI	0.03(0.001–0.61)	**0.02**	0.01(0.00–0.31)	**0.007**
Satellite Nodule	24.97(0.91–474.91)	0.06		
Proliferation pattern	0.93(0.44–1.97)	0.85		
Arterial rim enhancement	0.34(0.001–181.42)	0.74		
Enhancement pattern	2.31(0.28–18.72)	0.44		
Peritumoral hypointensity on HBP	0.18(0.02–1.71)	0.14		

Notes: EpCAM+/GPC3+ (Group A); EpCAM−/GPC3+ (Group B); EpCAM+/GPC3− (Group C); EpCAM−/GPC3− (Group D). P value of ≤ 0.05 and values labeled in bold format indicates a statistically significant difference.
Abbreviations: AFP, alpha-Fetoprotein; MVI, microvascular invasion; HBP, Hepatobiliary phase; OR, odds ratio; CI, Confidence Intervals.

MVI and satellite nodule (odds ratios, 0.1[95% CI: 0.02, 0.46], 8.88 [95% CI: 2.19, 36.11], respectively; *p*-values of 0.003, and 0.002, respectively; Table 5) than EpCAM−/GPC3+ HCC. Compared with EpCAM+/GPC3− HCC, EpCAM −/GPC3+ HCC showed macrotrabecular and clear cell pattern, and arterial rim enhancement (odds ratios, 0.07[95% CI: 0.01, 0.91], 15.82 [95% CI: 1.26, 199.44], respectively; *p*-values of 0.04, and 0.03, respectively; Table 5). For the differential diagnosis between four immune subtypes, separate and combined variables offered a wide range of sensitivity and specificity values (Table 6). The presence of all features resulted in sensitivities of 77.3% (95% CI: 0.659, 0.859), 83.3% (95% CI: 0.922, 1.000), and 90.9% (95% CI: 0.694, 0.984), and specificities of 67.7% (95% CI: 0.485, 0.827), 92.0% (95% CI: 0.828, 0.967), and 80.6% (95% CI: 0.619, 0.919), respectively.

Table 6 Diagnostic Performance of Significant Features and Combinations for Differentiating Immuosubtypes HCC

Variable Suggesting	AUC (95% CI)	Sensitivity (95% CI)	Specificity (95% CI)	PPV (95% CI)	NPV (95% CI)	ACC (95% CI)
A versus B						
MVI	0.666(0.550,0.783)	0.613(0.423,0.776)	0.720(0.603,0.815)	0.475(0.318,0.637)	0.818(0.700,0.899)	0.689(0.595,0.769)
Satellite nodule	0.628(0.508,0.747)	0.707(0.588,0.803)	0.548(0.363,0.722)	0.791(0.671,0.877)	0.436(0.282,0.602)	0.660(0.566,0.744)
Arterial rim enhancement	0.582(0.457,0.707)	0.907(0.811,0.958)	0.258(0.125,0.449)	0.747(0.643,0.830)	0.533(0.274,0.777)	0.717(0.625,0.794)
Arterial enhancement with wash-out	0.587(0.462,0.712)	0.880(0.780,0.940)	0.290(0.149,0.482)	0.750(0.644,0.834)	0.500(0.268,0.732)	0.708(0.615,0.786)
Peritumoral hypointensity on HBP	0.621(0.501,0.740)	0.548(0.363,0.722)	0.693(0.575,0.792)	0.425(0.274,0.590)	0.788(0.667,0.875)	0.651(0.556,0.735)
All five variables	0.802(0.712,0.888)	0.773(0.659,0.859)	0.677(0.485,0.827)	0.852(0.741,0.923)	0.553(0.385,0.710)	0.745(0.654,0.819)
B versus C						
Proliferation pattern	0.827(0.604,1.000)	0.667(0.241,0.940)	0.947(0.861,0.983)	0.500(0.174,0.826)	0.973(0.896,0.995)	0.926(0.845,0.969)
Arterial rim enhancement	0.703(0.449,0.958)	0.500(0.139,0.861)	0.907(0.811,0.958)	0.300(0.081,0.646)	0.958(0.873,0.989)	0.877(0.786,0.933)
Arterial enhancement with wash-out	0.701(0.450,0.952)	0.500(0.139,0.861)	0.893(0.795,0.950)	0.273(0.073,0.607)	0.957(0.872,0.989)	0.864(0.771,0.924)
All three variables	0.964(0.922,1.000)	0.833(0.365,0.991)	0.920(0.828,0.967)	0.455(0.181,0.754)	0.986(0.912,0.999)	0.914(0.830,0.960)
A versus D						
Tumor diameter (cm)	0.674(0.526,0.823)	0.682(0.451,0.853)	0.677(0.485,0.827)	0.600(0.389,0.782)	0.750(0.548,0.886)	0.679(0.545,0.790)
AFP (ng/mL)	0.825(0.706,0.943)	0.773(0.542,0.913)	0.806(0.619,0.919)	0.739(0.513,0.889)	0.833(0.645,0.937)	0.793(0.664,0.882)
Proliferation pattern	0.584(0.426,0.741)	0.136(0.036,0.360)	0.968(0.815,0.998)	0.750(0.219,0.987)	0.612(0.462,0.744)	0.623(0.388,0.741)
MVI	0.670(0.521,0.819)	0.613(0.423,0.776)	0.727(0.496,0.884)	0.760(0.545,0.898)	0.571(0.374,0.740)	0.660(0.526,0.774)
All four variables	0.889(0.794,0.984)	0.909(0.694,0.984)	0.806(0.619,0.919)	0.769(0.559,0.902)	0.926(0.742,0.987)	0.849(0.727,0.924)

Notes: EpCAM+/GPC3+ (Group A); EpCAM−/GPC3+ (Group B); EpCAM+/GPC3− (Group C); EpCAM−/GPC3− (Group D).
Abbreviations: AUC, area under curve; ACC, accuracy; NPV, negative predictive value; PPV, positive predictive value; MVI, microvascular invasion; AFP, alpha-fetoprotein.

https://doi.org/10.2147/IJGM.S502309

Discussion

In this work, we utilized MRI parameters to identify EpCAM and GPC3 expression in HCC lesions and linked MRI parameters with histological tests of the patients. The demand for biomarkers that can detect early relapse from primary tumor samples obtained from biopsy and images has increased due to the growing application of curative non-surgical therapies such as microwave ablation or percutaneous RFA.[19] It is well known that EpCAM is the primary cause of HCC relapse, metastasis, and prognosis,[4] positively staining for progenitor cell markers and downregulating hepatocyte differentiation.[20,21] GPC3 is implicated in HCC cell migration, which contributes to a poor prognosis and shows promotional effects on tumor progression.[8,22,23] Therefore, expression of EpCAM and GPC3 has been associated with aggressive behaviors and worse prognosis.[8,24] It would be therapeutically essential to identify imaging parameters that would distinguish HCC with aggressive features from in terms of predicting tumor response to anti-cancer therapy, and stratifying prognosis.[7,17] However, the results were still highly debatable.[17,18] Our study demonstrated that among clinicopathological and MR imaging findings, higher AFP serum level, macrotrabecular pattern, presence of MVI, arterial rim enhancement, and enhancement patterns were significant independent variables for potentially differentiating aggressive subtypes of HCC.

HCC is more prevalent in male patients than in females, which may be due to the fact that male patients are more likely to be exposed to risk factors such as HBV and HCV. We assume that androgen may be involved in the tumorigenicity of HCC and the high expression of EpCAM.[25] In our study, elderly patients often exhibited negative expressions of EpCAM and/or GPC3 in HCC, particularly in those with EpCAM−/GPC3−. Negative expression tumors in older patients tend to grow more slowly due to their favorable histologic characteristics.[17,23] In the present investigation, tumors larger than 4 cm were rarely seen in HCC patients with positive expression of EpCAM or GPC3 ($P > 0.05$). Whether tumor growth and differentiation are associated with EpCAM requires further study.[26] The prognosis and tumor biology of HCC patients are closely associated with the secretion of AFP and PIVKA-II, which independently predict HCC with aggressive features.[7,17,27] In this study, GPC3+ and EpCAM+ HCC had higher circulating levels of serum AFP ($P < 0.05$), suggesting a possible association between the immunological subtype of HCC and serum AFP values.

There is a correlation between Edmondson-Steiner grading and tumor subtype,[28] this correlation was not evident in our study ($P > 0.05$). HCC invasion and metastasis more frequently manifest as barrier collapse, absence of enhancing envelope, and presence of peritumoral arterial enhancement,[29–31] which is similar to our findings but not statistically significant ($P > 0.05$). In addition to this, MVI is more common in these immune subtypes of tumors as well as in HCC with a progenitor cell phenotype, suggesting more aggressive behavior,[32] and EpCAM+ or/and GPC3+ subtype of HCC are positively correlated with the onset of MVI. This diversity of invasive behavior may be related to many physiological features, including differentiation, proliferation, and angiogenesis.[32] Angiogenesis is one of the crucial factors of tumor growth and metastasis, and it is assumed to have a role in managing the behavior of HCC, and it may provide benefit to the EpCAM+ HCC for anti-angiogenesis therapy.[3]

The growth type has been attributed to multiple clinical-pathological progressions in HCCs. For example, the multifocal nodular confluent and infiltrative types are more invasive, and relatively higher EpCAM and GPC3 expression.[1,33] The study yielded the same results (EpCAM+ proportions of 32.4% and 18.9%, respectively) as the previous report if single nodules and simple nodules with extranodal growth were taken into account.[17] As early HCC tumors metastasize, they substitute the surrounding parenchyma, resulting in an undefined border.[34] In this study, the frequency of blurred margins and irregularly shaped tumors was higher in EpCAM-/GPC3+ HCC. It had no statistical significance, owing to large difference in cases among the four subtype groups. Also, satellite nodules and macrotrabecular patterns are one of the infiltrative manifestations of HCC and are considered as markers of aggressiveness.[35,36] As an independent predictor of both early and overall recurrence, this phenotype is linked to unfavorable prognostic factors including tumor volume, serum AFP level, vascular invasion, and satellite nodules.[36] In our findings, GPC3+ HCC showed high-frequency macrotrabecular architecture ($P < 0.05$).

In most cases, HCC is diagnosed primarily by imaging without histologic examination.[37] Aggressive HCC is indicated by the following imaging biomarkers: larger size, multifocality, non-smooth margin indicating extranodular growth from simple nodules, multifocal nodular confluence, and infiltrative type. These biomarkers may also detect HCC with poor differentiation and the existence of microvascular or macrovascular invasion.[33] Recognizing the relationship

between imaging variables and the histopathological and IHC features of HCC lesions may help with treatment criteria in individuals who have not undergone a biopsy. Gadoxetic acid-enhanced MRI is unquestionably acknowledged to exhibit the potential to be an imaging biomarker that is highly related to gene/protein expression and offers crucial roles in prognostication or offering tailored treatment.[38]

Additionally, compared to HCC with negative EpCAM, HCC with positive EpCAM were invariably accompanied by intratumoral bleeding (91.9%). We assume that this may be related to the pathological finding that only EpCAM+ cells were associated with higher angiogenesis levels and produced substantial hypervascular tumors.[31,32] It's been noted that GPC3 expression is linked to angiogenesis, which is more likely to happen in minute interior hemorrhages of HCC.[38] GPC3-positively expressing HCC shows arterial enhancement with a washout pattern more frequently on imaging. Tumors originating from hepatocytes show more early washout or are more likely to have atypical enhancement patterns as tumor grading progresses.[39] Since 66 cases of EpCAM−/GPC3+ subtypes displayed arterial enhancement with wash-out, it would be necessary to confirm the true biological significance of the association between EpCAM or GPC3 expression and enhancement pattern.

An earlier study supports that HCC with progenitor cell markers is more likely to display arterial rim enhancement.[33] Marginal enhancement patterns are more common in highly aggressive HCC as well as in atypical HCC, and are often associated with poor differentiation and poorer prognosis in HCC.[31] Multiple studies[16,40] have indicated that infiltrative growth, the existence of microvascular invasion may be associated with the rim enhancement of HCC. This implies that margin enhancement may be relevant to the identification of histopathological features and aggressive tumor behavior. Further, it may be employed as a viable noninvasive biomarker for HCC with poor prognoses that exhibit distinctive pathologic characteristics.[31] Marginal enhancement was more frequent in EpCAM+/GPC3+ HCC and progressed least in EpCAM-/GPC3- HCC. This study confirmed findings from earlier research. Thus, intensification of arterial margins is thought to be associated with aggressive behavior of HCC, but this still requires additional testing, including biopsy, to confirm the diagnosis.[31]

The ability of HBP to detect minor HCC lesions and distinguish pathologically early HCC from other malignant tumors is considered to offer the greatest improvement in prognosis.[41] An unfavorable prognosis and the expression of aggressive immunomarkers are identified in HCC with reduced signal intensities on HBP and elevated AFP.[8] Hyperintense HCC on HBP of EOB-MRI demonstrates weaker tumor marker expression, including EpCAM and GPC3.[23,42] It is possible that high-density HCC expresses fewer adverse prognostic markers. This is not reflected in the results of the present study, possibly because the limited number of sample cases reduces the validity. We found that the use of peritumoral hypodensity on HBP could distinguish between positive and negative EpCAM expression in malignant tumors and help to differentiate HCC subtypes.

In this study, MRI parameters displayed potential as a non-invasive method for evaluating the histopathological and immune characteristics of HCC lesions. Nevertheless, we contend that MRI parameters are insufficient to entirely replace IHC evaluation in HCC. By offering complementary and extra information on tumor features at the whole-tumor level, the MRI parameters analysis might be utilized to corroborate the identification of HCC lesions in biopsied or excised samples.[13] Univariate and multivariate logistic regression analysis results indicate valuable assessment in predicting the aggressiveness of HCC. According to the immunological subclassification, the multivariate analysis further revealed that MVI, satellite nodule, proliferation pattern, arterial rim enhancement, tumor size, and AFP level were independent predictors of the immune subtypes of HCC. These findings supported that the tumor aggressiveness was directly correlated with the tumor appearance and pathological status. Among MR imaging results, arterial peripheral enhancement, arterial enhancement with wash-out pattern, and peritumoral hypointensity on HBP images were identified as crucial distinct variables that had the potential to predict immune subtypes of HCC. Combining some of these criteria resulted in greater specificity (92.0% for three and 80.6% for four), which could be considered reliable for differentiating immune subtypes of HCC.

This study has some limitations. First of all, because of the retrospective design, selection bias is inevitable. Despite this study having a relatively large sample of EpCAM and GPC3 HCC, the number of enrolled EpCAM+/GPC3− patients (6 patients [4.4%]) is particularly small. The disease rarity may be the cause, and the uneven sample size may have affected the accuracy of the diagnosis. Moreover, tumor resection was performed on every case under consideration;

no biopsy or transplant specimens were included. Thus, the general relevance of the study's results to all clinical conditions may be compromised. Further, this retrospective study was conducted at a single center, without any external verification being carried out. To completely evaluate the prognostic value of our immunosubtype model in HCC patients, huge sample sizes and a standardized multicenter collaborative study are still necessary. This immune classification model has the potential to demonstrate the significance of risk distribution for HCC patients. By providing optimal medical evidence, it can develop a standardized set of criteria that can be widely accepted. As a final precaution, we avoid functional MR imaging and radiomics analysis, both of which necessitate the use of specialized software for measurement and have drawbacks including difficulty in interpreting and poor practical clinical implementation.

Conclusions

In conclusion, this study echoed the relationship between HCC with EpCAM or GPC3 expression and MR features and highlighted the value of MR and AFP as biomarkers for aggressive HCC that can be assessed noninvasively through imaging features and AFP values. It was not possible to find any similar phenomena between EpCAM−/GPC3+ and EpCAM−/GPC3− HCCs. Second, although MRI parameters show potential as a noninvasive method to assess the histopathologic and immunologic features of HCC lesions, the parameters are not sufficient to completely replace IHC for the assessment of HCC. This suggests that prospective validation and a larger sample size are necessary to explore the impact of these molecular subtypes on the risk stratification of HCC patients and their role in personalized management.

Abbreviations

HCC, Hepatocellular carcinoma; EpCAM, epithelial cell adhesion molecule; GPC3, Glypican-3; AFP, alpha-fetoprotein; PIVKA-II, Protein induced by Vitamin K absence or antagonists-II; MRI, Magnetic resonance imaging; GD-EOB-DTPA, Gadolinium-ethoxybenzyl-diethylenetriamine pentaacetic acid; AP, Arterial phase; PVP, Portal venous phases; DP, Delayed phases; HBP, Hepatobiliary phase; T1WI, T1-weighted imaging; T2WI, T2-weighted imaging; MVI, microvascular invasion; PPV, Positive predictive value; NPV, Negative predictive value; CI, Confidence interval.

Data Sharing Statement

The datasets used and/or analyzed during the present study are available from the corresponding author on reasonable request.

Ethics Approval

The present study was approved by the Ethics Committee of Minhang Hospital, Fudan University and written informed consent was provided by all patients prior to the study start. All procedures were performed in accordance with the ethical standards of the Institutional Review Board and The Declaration of Helsinki, and its later amendments or comparable ethical standards.

Disclosure

The authors report no conflicts of interest in this work.

References

1. Zhao J, Gao S, Sun W, et al. Magnetic resonance imaging and diffusion-weighted imaging-based histogram analyses in predicting glypican 3-positive hepatocellular carcinoma. *Eur J Radiol*. 2021;139:109732. PMID: 33905978. doi:10.1016/j.ejrad.2021.109732
2. Bray F, Ferlay J, Soerjomataram I, Siegel RL, Torre LA, Jemal A. Global cancer statistics 2018: GLOBOCAN estimates of incidence and mortality worldwide for 36 cancers in 185 countries. *CA Cancer J Clin*. 2018;68(6):394–424. PMID: 30207593. doi:10.3322/caac.21492
3. Jeng KS, Chang CF, Sheen IS, Jeng CJ, Wang CH. Cellular and molecular biology of cancer stem cells of hepatocellular carcinoma. *Int J mol Sci*. 2023;24(2):1417. PMID: 36674932. doi:10.3390/ijms24021417
4. Chen VL, Huang Q, Harouaka R, et al. A dual-filtration system for single-cell sequencing of circulating tumor cells and clusters in HCC. *Hepatol Commun*. 2022;6(6):1482–1491. PMID: 35068084. doi:10.1002/hep4.1900
5. Nicolosi A, Gaia S, Risso A, et al. Serum glypican-3 for the prediction of survival in patients with hepatocellular carcinoma. *Minerva Gastroenterol*. 2022;68(4):378–386. PMID: 36222678. doi:10.23736/S2724-5985.21.03006-0

6. Li D, Lin S, Hong J, Ho M. Immunotherapy for hepatobiliary cancers: emerging targets and translational advances. *Adv Cancer Res*. 2022;156:415–449. PMID: 35961708. doi:10.1016/bs.acr.2022.01.013
7. Wang Y, Guo J, Ma D, et al. Reduced tumor stiffness quantified by tomoelastography as a predictive marker for glypican-3-positive hepatocellular carcinoma. *Front Oncol*. 2022;12:962272. PMID: 36518314. doi:10.3389/fonc.2022.962272
8. Jiang D, Zhang Y, Wang Y, Xu F, Liang J, Wang W. Diagnostic accuracy and prognostic significance of Glypican-3 in hepatocellular carcinoma: a systematic review and meta-analysis. *Front Oncol*. 2022;12:1012418. PMID: 36212469. doi:10.3389/fonc.2022.1012418
9. Borde T, Nezami N, Laage Gaupp F, et al. Optimization of the BCLC staging system for locoregional therapy for hepatocellular carcinoma by using quantitative tumor burden imaging biomarkers at MRI. *Radiology*. 2022;304(1):228–237. PMID: 35412368. doi:10.1148/radiol.212426
10. Jain D. Tissue diagnosis of hepatocellular carcinoma. *J Clin Exp Hepatol*. 2014;4(Suppl 3):S67–73. PMID: 25755614. doi:10.1016/j.jceh.2014.03.047
11. Singal AG, Reig M, Villanueva A. Emerging tools for hepatocellular carcinoma surveillance. *Am J Gastroenterol*. 2022;117(12):1948–1951. PMID: 36114768. doi:10.14309/ajg.0000000000002015
12. Karaoğullarindan Ü, Gümürdülü Y, Üsküdar O, et al. Prognostic value and morphological findings of overexpression of glypican-3 in hepatocellular carcinoma. *Eur J Gastroenterol Hepatol*. 2023;35(1):89–93. PMID: 36165051. doi:10.1097/MEG.0000000000002452
13. Dong SY, Wang WT, Chen XS, et al. Microvascular invasion of small hepatocellular carcinoma can be preoperatively predicted by the 3D quantification of MRI. *Eur Radiol*. 2022;32(6):4198–4209. PMID: 35079885. doi:10.1007/s00330-021-08495-4
14. Hectors SJ, Wagner M, Bane O, et al. Quantification of hepatocellular carcinoma heterogeneity with multiparametric magnetic resonance imaging. *Sci Rep*. 2017;7(1):2452. PMID: 28550313. doi:10.1038/s41598-017-02706-z
15. Friemel J, Rechsteiner M, Frick L, et al. Intratumor heterogeneity in hepatocellular carcinoma. *Clin Cancer Res*. 2015;21(8):1951–1961. PMID: 25248380. doi:10.1158/1078-0432.CCR-14-0122
16. Choi SY, Kim SH, Park CK, et al. Imaging features of gadoxetic acid-enhanced and diffusion-weighted MR imaging for identifying cytokeratin 19-positive hepatocellular carcinoma: a retrospective observational study. *Radiology*. 2018;286(3):897–908. PMID: 29166246. doi:10.1148/radiol.2017162846
17. Chen J, Wu Z, Xia C, et al. Noninvasive prediction of HCC with progenitor phenotype based on gadoxetic acid-enhanced MRI. *Eur Radiol*. 2020;30(2):1232–1242. PMID: 31529254. doi:10.1007/s00330-019-06414-2
18. Hu XX, Wang WT, Yang L, et al. MR features based on LI-RADS identify cytokeratin 19 status of hepatocellular carcinomas. *Eur J Radiol*. 2019;113:7–14. PMID: 30927962. doi:10.1016/j.ejrad.2019.01.036
19. Cheng KC, Ho KM. Pure laparoscopic liver resection versus percutaneous radiofrequency ablation for small hepatocellular carcinoma: a propensity score and multivariate analysis. *Transl Cancer Res*. 2022;11(1):43–51. PMID: 35261883. doi:10.21037/tcr-21-1045
20. Karagonlar ZF, Akbari S, Karabicici M, et al. A novel function for KLF4 in modulating the De-differentiation of EpCAM-/CD133- nonStem Cells into EpCAM+/CD133+ Liver Cancer Stem Cells in HCC Cell Line HuH7. *Cells*. 2020;9(5):1198. PMID: 32408542. doi:10.3390/cells9051198
21. Park DJ, Sung PS, Kim JH, et al. EpCAM-high liver cancer stem cells resist natural killer cell-mediated cytotoxicity by upregulating CEACAM1. *J Immunother Cancer*. 2020;8(1):e000301. PMID: 32221015. doi:10.1136/jitc-2019-000301
22. Gu D, Xie Y, Wei J, et al. MRI-based radiomics signature: a potential biomarker for identifying glypican 3-positive hepatocellular carcinoma. *J Magn Reson Imaging*. 2020;52(6):1679–1687. PMID: 32491239. doi:10.1002/jmri.27199
23. Chen Y, Qin Y, Wu Y, et al. Preoperative prediction of glypican-3 positive expression in solitary hepatocellular carcinoma on gadoxetate-disodium enhanced magnetic resonance imaging. *Front Immunol*. 2022;13:973153. PMID: 36091074. doi:10.3389/fimmu.2022.973153
24. Ortiz MV, Roberts SS, Glade Bender J, Shukla N, Wexler LH. Immunotherapeutic targeting of GPC3 in pediatric solid embryonal tumors. *Front Oncol*. 2019;9:108. PMID: 30873384. doi:10.3389/fonc.2019.00108
25. Lai HC, Chung WM, Chang CM, et al. Androgen receptor enhances the efficacy of sorafenib against hepatocellular carcinoma through enriched EpCAM stemness. *Anticancer Res*. 2020;40(3):1285–1295. PMID: 32132025. doi:10.21873/anticanres.14070
26. Chan AW, Tong JH, Chan SL, Lai PB, To KF. Expression of stemness markers (CD133 and EpCAM) in prognostication of hepatocellular carcinoma. *Histopathology*. 2014;64(7):935–950. PMID: 24506513. doi:10.1111/his.12342
27. Jang TY, Dai CY. Cutoff values of protein induced by vitamin K absence or antagonist II for diagnosing hepatocellular carcinoma. *Medicine*. 2022;101(39):e30936. PMID: 36181046. doi:10.1097/MD.0000000000030936
28. Chang YS, Chou YP, Chung CC, et al. Molecular classification of hepatocellular carcinoma using Wnt-Hippo signaling pathway-related genes. *Cancers*. 2022;14(19):4580. PMID: 36230503. doi:10.3390/cancers14194580
29. Öcal O, Ingrisch M, Ümütlü MR, et al. Prognostic value of baseline imaging and clinical features in patients with advanced hepatocellular carcinoma. *Br J Cancer*. 2022;126(2):211–218. PMID: 34686780. doi:10.1038/s41416-021-01577-6
30. Wang H, Yang C, Rao S, et al. MR imaging of hepatocellular adenomas on genotype-phenotype classification: a report from China. *Eur J Radiol*. 2018;100:135–141. PMID: 29496071. doi:10.1016/j.ejrad.2018.01.023
31. Rhee H, An C, Kim HY, Yoo JE, Park YN, Kim MJ. Hepatocellular carcinoma with irregular rim-like arterial phase hyperenhancement: more aggressive pathologic features. *Liver Cancer*. 2019;8(1):24–40. PMID: 30815393. doi:10.1159/000488540
32. Shan YF, Huang YL, Xie YK, et al. Angiogenesis and clinicopathologic characteristics in different hepatocellular carcinoma subtypes defined by EpCAM and α-fetoprotein expression status. *Med Oncol*. 2011;28(4):1012–1016. PMID: 20571936. doi:10.1007/s12032-010-9600-6
33. Jeong HT, Kim MJ, Kim YE, Park YN, Choi GH, Choi JS. MRI features of hepatocellular carcinoma expressing progenitor cell markers. *Liver Int*. 2012;32(3):430–440. PMID: 22097930. doi:10.1111/j.1478-3231.2011.02640.x
34. Cho ES, Choi JY. MRI features of hepatocellular carcinoma related to biological behavior. *Korean J Radiol*. 2015;16(3):449–464. PMID: 25995679. doi:10.3348/kjr.2015.16.3.449
35. Vernuccio F, Porrello G, Cannella R, et al. Benign and malignant mimickers of infiltrative hepatocellular carcinoma: tips and tricks for differential diagnosis on CT and MRI. *Clin Imaging*. 2021;70:33–45. PMID: 33120287. doi:10.1016/j.clinimag.2020.10.011
36. Ziol M, Poté N, Amaddeo G, et al. Macrotrabecular-massive hepatocellular carcinoma: a distinctive histological subtype with clinical relevance. *Hepatology*. 2018;68(1):103–112. PMID: 29281854. doi:10.1002/hep.29762
37. McEvoy SH, McCarthy CJ, Lavelle LP, et al. Hepatocellular carcinoma: illustrated guide to systematic radiologic diagnosis and staging according to guidelines of the American Association for the Study of Liver Diseases. *Radiographics*. 2013;33(6):1653–1668. PMID: 24108556. doi:10.1148/rg.336125104

38. Chen R, Bai Y, Liu T, et al. Evaluation of glypican-3 expression in hepatocellular carcinoma by using IDEAL IQ magnetic resonance imaging. *Acad Radiol*. 2021;28(8):e227–e234. PMID: 32540197. doi:10.1016/j.acra.2020.05.015
39. Lee JH, Lee JM, Kim SJ, et al. Enhancement patterns of hepatocellular carcinomas on multiphasic multidetector row CT: comparison with pathological differentiation. *Br J Radiol*. 2012;85(1017):e573–83. PMID: 22919011. doi:10.1259/bjr/86767895
40. Miltiadous O, Sia D, Hoshida Y, et al. Progenitor cell markers predict the outcome of patients with hepatocellular carcinoma beyond Milan criteria undergoing liver transplantation. *J Hepatol*. 2015;63(6):1368–1377. PMID: 26220754. doi:10.1016/j.jhep.2015.07.025
41. Chong H, Gong Y, Zhang Y, Dai Y, Sheng R, Zeng M. Radiomics on gadoxetate disodium-enhanced MRI: non-invasively identifying glypican 3-positive hepatocellular carcinoma and postoperative recurrence. *Acad Radiol*. 2023;30(1):49–63. PMID: 35562264. doi:10.1016/j.acra.2022.04.006
42. Yoneda N, Matsui O, Kobayashi S, et al. Current status of imaging biomarkers predicting the biological nature of hepatocellular carcinoma. *Jpn J Radiol*. 2019;37(3):191–208. PMID: 30712167. doi:10.1007/s11604-019-00817-3